

# Multiple Eye Disease Detection using Hybrid Adaptive Mutation Swarm Optimization and RNN

P. Glaret Subin<sup>1</sup>, P. Muthu Kannan<sup>2</sup>

Department of ECE, Saveetha School of Engineering, Saveetha Institute of Medical and Technical Sciences  
Chennai-602105, India.<sup>1,2</sup>

Department of ECE, College of Engineering and Technology, SRM Institute of Science and Technology, Vadapalani Campus  
Chennai- 600026, India<sup>1</sup>

**Abstract**—The major cause of visual impairment in aged people is due to age related eye diseases such as cataract, diabetic retinopathy, and glaucoma. Early detection of eye diseases is necessary for better diagnosis. This paper concentrates on the early identification of various eye disorders such as cataract, diabetic retinopathy, and glaucoma from retinal fundus images. The proposed method focuses on the automated early detection of multiple diseases using hybrid adaptive mutation swarm optimization and regression neural networks (AED-HSR). In the proposed work, the input images are preprocessed and then multiple features such as entropy, mean, color, intensity, standard deviation, and statistics are extracted from the collected data. The extracted features are segmented by using an adaptive mutation swarm optimization (AMSO) algorithm to segment the disease sector from the fundus image. Finally, the features collected are fed to a regression neural network (RNN) classifier to classify each fundus image as normal or abnormal. If the classifier output is abnormal, then it is classified by the corresponding diseases in terms of cataract, glaucoma, and diabetic retinopathy, which improves the accuracy of detection and classification. Ultimately, the results of the classifiers are evaluated by several performance analyses and the viability of structural and functional features is considered. The proposed system predicts the type of the disease with an accuracy of 0.9808, specificity of 0.9934, sensitivity of 0.9803 and F1 score of 0.9861 respectively.

**Keywords**—Adaptive mutation swarm optimization; fundus image; feature extraction; RNN classifier; standard deviation

## I. INTRODUCTION

Nowadays, aged people are mostly affected by chronic diseases such as cataract, glaucoma and diabetic retinopathy, which lead to visual impairment. The optic nerve is damaged due to glaucoma, which results in loss of vision. Glaucoma occurs due to a slow rise in the normal fluid pressure inside the eyes. Cataract occurs due to the clouding of the eye's lens. The progressive damage in the retina's blood vessels, which are essential for good vision of the eye, leads to Diabetic Retinopathy [1]. Based on the supervised learning method, blood vessels are segmented from the fundus image that can be done using Zernike moment-based Shape descriptors and training can be performed using an ANN-based binary classifier to predict cardio vascular diseases [2]. Multiple instances A learning technique is used to classify the diseased image and healthy image, in which the classification can be done by binary classification [3]. Microaneurysms can be recognized using principal component analysis, morphological

processing, averaging filter, and support vector machine classifier. Diabetic Retinopathy disease can also be identified [4]. The early signs of diabetic retinopathy can be identified by applying nineteen features extracted from the fundus image to an artificial neural network, which is trained by Levenberg-Marquardt, and the disease is classified by using Bayesian Regularization [5]. Red lesions can be detected in the blood vessels by using a Gaussian filter and the disease can be predicted using an SVM classifier [6]. Based on the singular value decomposition algorithm, dictionary learning methods can be used to classify healthy people from diabetic patients based on singular Value Decomposition Algorithm [7]. The fundus image is segmented by using a Deep Convolution Neural Network and it increases the accuracy and efficiency in predicting non-proliferated diabetic retinopathy [8]. The blood vessels can be segmented by using dilated convolution, which leads to more accurate detection of ophthalmologic diseases [9]. The two filtering methods, namely median filtering and Gaussian derivative filtering, are used to define the bifurcation point of a blood vessel image segment [10]. DR (Diabetic Retinopathy) can be recognized using the ANN classifier and region growing segmentation to extract exudates, optic plate and veins from the fundus images [11]. DR can be detected by using a reformed capsule network, which attains an accuracy of 97.98% [12]. A hierarchical severe grading system model was developed to detect and classify the different grades of DR. The classifier accuracy is 94% [13]. The optic disc and optic cup boundary of the fundus images are segmented and by using Weighted Least Square fit, holistic features and disc ratio are extracted, and then they are fed to a Convolutional Multi-Layer Neural Network Classifier to classify the glaucoma [14]. A classification method of multi feature analysis along with a Discrete Wavelet transform is used to detect glaucoma. This model classifies glaucoma with an accuracy of 95% [15]. The input fundus image is validated using Le-Net architecture and the optic disc and optic cup are segmented using U-Net Architecture. Glaucoma can be detected with the use of SVM Classifier, Neural Network Classifier, and Adaboost Classifiers [16]. The eyeball area is extracted from the fundus image using an object detection network and multi task learning is applied to detect the cataract [17]. A Deep Convolution Neural Network with Resnet for classification can be used to identify cataract. The systems show an accuracy of 95.77% [18]. Gray Level Co-occurrence Matrix is utilized for feature extraction, and the classification of different levels of cataract can be done by Back Propagation Neural Network Classifier. This system

provides an accuracy of 82.4% [19]. The above-mentioned techniques are utilized to anticipate a single disease from the fundus image of the retina. The proposed paper uses hybrid adaptive mutation swarm optimization and regression neural network (AED-HSR) to provide automated early detection of multiple diseases.

The contributions of the proposed work are:

- Multiple features are extracted from the collected data and standard deviation, smoothness, entropy, shape, color, intensity and statistics are included for feature extraction.
- An adaptive mutation swarm optimization (AMSO) algorithm is used to segment the disease sector from fundus image.
- The collected features are fed to the regression neural network-based classifier to classify each fundus image as normal or abnormal.

The rest of this paper provides the recent related works under Section II, Problem methodology and System model in Section III, the proposed AED-HSR technique using AMSO algorithm and RNN algorithm experimental setup and results are explained in Section IV, and Section V describes the conclusion of AED-HSR.

## II. RELATED WORKS

Kangrok et al., proposed a strategy to detect DR by utilizing automatic segmentation of the ETDRS 7SF in order to expel the undesirable components in the fundus image, and then it was fed to a ResNet – 34 model for the classification of the disease, which provided an accuracy of 83.38% [20]. Saeid et al., proposed a combinational approach of fuzzy C-means and genetic algorithms for the prediction of DR from the angiographic images of diabetic patients, which provided a sensitivity of 78% [21]. Zhuang et al., introduced a weighted voting algorithm to categorize the DR disease and the trained network model was applied to the hospital data, which provided 92% accuracy [22]. Rego et al., worked on a Convolutional Neural Network (CNN) model with Inception-V3 for DR screening of fundus images. In this approach, the model analyzed 295 images and the results were compared with a team of ophthalmologists. This model predicted DR with an accuracy of 95% [23]. Mohammed Hasan et al., suggested a combined method of Convolution Neural Network and Principal Component Analysis for the diagnosis of DR with an accuracy of 98.44% [24]. Hemelings et al., suggested a method based on a deep learning approach to identify glaucoma in which the fundus image was cropped with radius as image size percentage, optic nerve head (ONH) centered with spacing of 10–60%. This model resulted in an AUC of 0.94 [25]. Salam et al., developed an algorithm for glaucoma diagnosis based on combined structural and non-structural features. This method was evaluated with 100 patients' fundus images, which provided a 100% sensitivity and an 87% specificity [26]. Nataraj et al., suggested a machine learning based classification technique to identify glaucoma from fundus images. This method used a unique template approach for segmentation, the Gray Level Coherence Matrix approach

for feature extraction, and wavelet transform for texture and structure-based features to improve the efficiency of the system [27]. Latif et al., proposed a model for detecting glaucoma that had two parts: one to find the optic discs and the other to use transfer learning to find glaucoma. This method provided 95.75% accuracy, 94.75% sensitivity, and 94.90% specificity [28]. Xu et al., proposed a method based on the transfer induced attention network for glaucoma diagnosis that extracted the deep patterns related to disease with limited supervision. The model was evaluated on clinical datasets, which provided an accuracy of 85.7% [29]. A novel method was developed by Raja et al., to identify glaucoma at an earlier stage by using a deep learning approach for segmenting the optic cup and optic disc and an SVM classifier to predict the disease with 92% accuracy [30]. Hasan et al., suggested a convolution neural network to diagnose the cataract disease from the fundus image. This model predicted the cataract disease with an accuracy of 98.17% [31]. Azhar et al., employed CNN for extracting the features and Support Vector Machine (SVM) for the prediction of cataracts. The system model provided an accuracy of 95.65% [32]. Pratap et al., suggested a technique for automatic cataract detection by utilizing singular value decomposition as a feature extractor and SVM as a classifier. The accuracy of the method was 97.78% [33]. Imran et al., developed a strategy for the identification of cataracts. The fundus images were preprocessed and then, by using the combination of Self Organizing Maps and Radial Basis Function (RBF) Neural Network, the model predicted the cataract with an accuracy of 95.3% [34]. Behera et al., [35] used an RBF-based SVM Classifier to predict cataract diseases from fundus images.

## III. METHODOLOGY

The proposed automated early detection of multiple eye diseases by means of hybrid adaptive mutation swarm optimization and regression neural network (AED-HSR) techniques has been used to improve the accuracy of eye disease diagnosis. The proposed system consists of two phases. In the first phase, AMSO is used to segment the blood vessels, optic distance, exudates, and hemorrhage from the extracted features of the preprocessed fundus image. In the second phase, an RNN classifier is utilized to identify multiple eye diseases, namely cataract, diabetic retinopathy, and glaucoma. The flow diagram for the proposed system model for multiple disease detection is shown in Fig. 1.

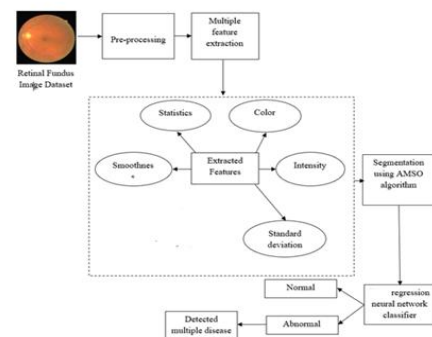


Fig. 1. System Model of Proposed AED-HSR Technique.

### A. Preprocessing

The creation of a binary mask is the initial step in image preprocessing, which is used to recognize that the pixels belong to the Region of Interest. Creating a binary mask avoids unwanted processing of pixels outside the ROI, which will reduce the processing time of an image. Masking can be done by convoluting the red color channel with a Gaussian low pass filter. Then the image undergoes thresholding by using Otsu's global thresholding [36]. The image is then converted to a grayscale image, which has better contrast than the other color channels, such as the red color channel and blue color channel. Since various eye diseases can be identified in the blood vessels of the fundus image, and the contrast between the blood vessels can be easily identified in the green channel of the color image. After the conversion of the grayscale image, the image is resized to standard form because of the wider size of the input image. The resized image is then denoised using a gray level morphological operation to remove the brightness strip located at the center of the blood vessels.

### B. Feature Extraction

Feature extraction is a method of mapping the primary feature into a low dimensional feature space for better classification. Each feature should have a larger variance to distinguish the features from the image. To detect the diseased image, the features such as blood vessels, optic disc, hemorrhage, and retinal exudates should be extracted from the fundus image of the retina. Glaucoma can be identified by the variation in the optic cup, which is a portion of the optic disc. In order to accomplish the automatic diagnosis of glaucoma, the location of the optic disc, which contains more information for glaucoma detection, must be extracted from the fundus image [37]. Optic disc feature extraction can be done by the entropy method. Blood vessels are extracted by using Gabor filters [38].

1) *Entropy*: The average quantity of information owing to the variance of pixel values in an image is defined as entropy in image processing. The image entropy of a distinct brightness values can be calculated by "1"

$$H(I) = \sum_{k=1}^{B_g} P(I_k) \log_2 \left( \frac{1}{P(I_k)} \right) \quad (1)$$

where  $P(I_k)$  denotes the  $k$  brightness value distribution of image  $I$  and  $B_g$  represents the number of brightness levels in an image.

Based on the values of entropy, texture analysis of an image can be done. Lower values of entropy result in the smoothening of texture, whereas higher values of entropy give texture with more details. In the proposed model, higher values of entropy in the fundus image are taken as the optic disc location as it has more details such as nerves and blood vessels.

2) *Gabor filters*: Gabor filters are mostly used to enhance the blood vessels from the fundus image. The product of Gaussian envelope function and complex trigonometric function results in complex Gabor function. To enhance the blood vessels in the fundus image, real portion of the complex Gabor function is utilized and is given by "2"

$$S(u,v,\lambda,\phi,\sigma,\tau) = \exp\left(\frac{-u^2 - v^2 - \tau^2}{2\sigma^2}\right) \cdot \cos(2\pi u' / \lambda + \phi) \quad (2)$$

where  $s$  represents the two-dimensional Gabor kernel function with variables  $u$  and  $v$  and  $u' = u \cos \phi + v \sin \phi$  and  $v' = -u \sin \phi + v \cos \phi$ . Scale ( $\sigma$ ), Wavelength ( $\lambda$ ), orientation ( $\phi$ ) and aspect ratio ( $\tau$ ) are the four parameters to control the shape. The Gabor kernel is rotated at an angle of 15 degree so that 12 different kernels are obtained; it is convolved with the preprocessed image and it selects the utmost response for each pixel. Subsequently, the pixels having blood vessels are more prevailing than the other pixels.

The statistical features, namely mean and standard deviation can be calculated using the following equations "3" and "4"

$$\mu = \sum_{k=0}^{L-1} k p(k) \quad (3)$$

$$\sigma^2 = \sum_{k=0}^{L-1} (k - \mu)^2 p(k) \quad (4)$$

### C. Proposed AED-HSR Technique using AMSO and RNN Algorithm

In this section, AMSO is described in Section.4.1 and Regression neural network classifier to identify the diseased image is explained briefly in Section.4.2.

1) *Segmentation using AMSO algorithm*: The features retrieved from the fundus image are segmented using the Adaptive Mutation Swarm Optimization (AMSO) technique. Basically, Swarm will be initiated by the Particle Swarm Optimization. The solution of each search space is determined based on the position and the velocity of the particle in the swarm. The position and the velocity of the particle are changed for each iteration and the global best position  $p_g$  and personal best position  $p_i$  are found out. To reach the ideal PSO state, a larger interference amplitude is needed in the early iteration phase to ensure better global search capabilities and a smaller interference amplitude is required in the late iteration phase to ensure convergence.

a) *Chase-Swarming Behavior*: where  $x_i$  represents the position of cockroach, step denotes a fixed value, 'rand' represents a random number lying between 0 and 1,  $p_i$  is the personal best position, and  $p_g$  is the global best position. The personal best position of cockroach of size  $N$  is given by "5" and "6"

$$X_i = x_i + \text{step} \cdot \text{rand} \cdot (p_i - x_i), x_i \neq p_i \quad (5)$$

$$X_i = x_i + \text{step} \cdot \text{rand} \cdot (p_g - x_i), x_i = p_i \quad (6)$$

where visual is a constant,  $j = 1, 2, \dots, N$ ,  $i = 1, 2, \dots, N$ . The global best position of the cockroach is given by "7" and "8"

$$p_i = \text{opt}_j \{x_j | |x_i - x_j| \leq \text{Visual}\} \quad (7)$$

$$p_g = \text{opt} \{x_i\} \quad (8)$$

The inertial weight to chase swarming component of original AMSO is given by "9" and "10"

$$X_i = \omega \cdot x_i + \text{step} \cdot \text{rand} \cdot (p_i - x_i), x_i \neq p_i \quad (9)$$

$$X_i = \omega \cdot x_i + \text{step.rand.}(p_g - x_i), x_i = p_i \quad (10)$$

where  $\omega$  is an inertial weight of the particle.

*b) Hunger Behavior:* In this paper, an enhanced cockroach swarm optimization is prolonged with an extra feature called hunger behavior. For a particular period of time, when the cockroach is hungry, it migrates from its original position and searches for food source  $x_{\text{food}}$  within the search space. Partial differential equation (PDE) migration technique is used for hunger behaviour modelling. Hunger behaviour impedes local optimization and increases population diversity.

Kerckhove defines the PDE migration equation as

$$\partial p / \partial t = -s \partial p / \partial x \quad (11)$$

with initial population distribution  $p(0, x) = p_0(x)$ .

where the parameter  $s$  controls the migration speed.  $p$  represents population size,  $t$  denotes the time, and  $x$  represents the location or position.  $(t, x)$  is the population size at time  $t$  in location  $x$

Equation (9) can be expressed as

$$\partial p / \partial t + s \partial p / \partial x = 0 \quad (12)$$

By integration, we have

$$x - st = \sigma, p = p(\beta), p = p(x - st)$$

$$p[t, x] = p_0[x - st]$$

Since displacement is the product of speed and time, in  $p_0(x - st)$ ,  $p_0(x)$  is replaced by  $st$ .

$p_0(x - st)$ , satisfies PDE at any initial population distribution  $p_0(x)$ . Hunger behavior is defined as follows: If hunger is equal to threshold hunger  $t_{\text{hunger}}$ , then the new position of cockroach is

$$X_i = x_i + (x_i - st) + x_{\text{food}} \quad (13)$$

where  $x_i$  denotes the position of the cockroach,  $(x_i - st)$  represents the migrated position of the cockroach from its current position, and hunger is a random number which lies in the range of 0 to 1.

#### D. Classifying Feature Models using RNN

The segmented portions of the fundus images are fed into the Regression Neural Network Classifier for the prediction of diseases in the form of a regression task. The architecture of the RNN is shown in Fig. 2. The segmented features are given as input to the RNN, which contains a fully connected layer and batch normalization with a Leaky Rectified Linear Unit (FC-BN-LReLU), pursued by a dropout layer with a dropping probability of 0.2 to avoid the overfitting problems, and two layers of FC-BN-LReLU, followed by a drop out layer. The following layer is a fully connected layer with LReLU, which does not contain batch normalization. The last layer is a fully connected layer without any activation function that will classify the type of disease.

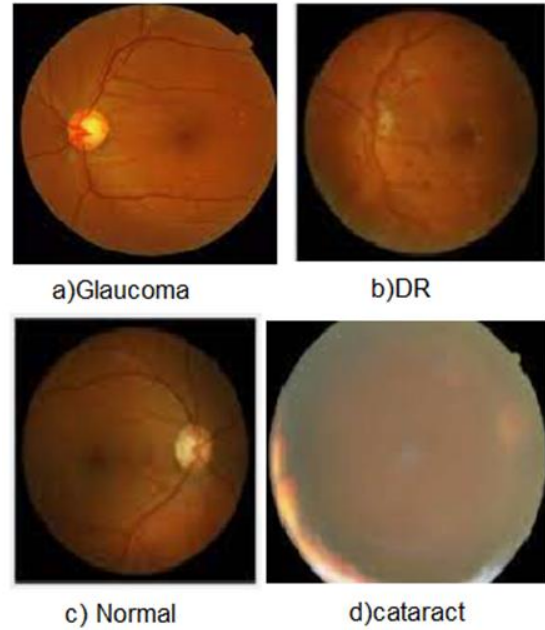


Fig. 2. Test Image Samples.

#### IV. EXPERIMENTAL SET-UP AND RESULTS

In the proposed AED-HSR, Cataract, glaucoma, DR and normal images are classified from the fundus images and the performance analysis is calculated based on distinct algorithms. The proposed method was implemented in the online datasets using MatlabR2022a.

##### A. Dataset

The proposed AED-HSR method was implemented on the dataset that comprised of 800 normal images, 800 cataract images, 800 diabetic retinopathy images, and 800 glaucoma images, taken from the Ocular Disease Intelligent Recognition (ODIR) database, which contains the ophthalmic database of 5000 patients, including their ages, right and left eye fundus images, and the doctor's diagnostic keywords. The images are collected by the Shanggong Medical Technology Co., Ltd. from numerous hospitals in China.

##### B. Results

In the experimental set-up, 30% of images are utilized for testing and 70% of images are utilized for training. The test image samples are shown in Fig. 2. A learning rate of 0.01 with a maximum of 39 epochs was used in the training phase of the proposed system. The proposed method utilizes 5 distinct features such as smoothness, statistics, color, intensity, and standard deviation to train the RNN. The training performance of the AED-HSR in terms of training, validation and test data is shown in Fig. 3. From the training progress of AED-HSR, the mean square error (MSE) drops rapidly in the first 10 epochs and the best validation performance is 0.074662 at epoch 33. The training MSE gradually drops a bit and the stability is more in the final epochs. In the training model, more attributes are used to aid in prediction which may be useful to prevent overfitting.

The training state of the proposed AED-HSR shown in Fig. 4 will provide the gradient of 0.16819 at epoch 39 and the maximum mu value of 0.001 is reached at epoch 39 which controls the neurons weight updating process during training. By applying the test images as an input to the model, AED-HSR classifies the image as a diseased image or normal image.

A regression analysis was performed in order to determine the relationship between the network output and the corresponding targets. The Regression plot of the AED -HSR model is shown in Fig. 5 which shows a correlation between the two sets of data. It demonstrates that there is a good fit between the values that were predicted by AED-HSR and the actual measured data with higher values of R. The regression plot indicates that the outputs closely match the targets with an R-Value. The Confusion matrix for the four different models is shown in Fig. 6. From the values of Confusion Matrix (VCM), True Positive (TP), True Negative, False Positive and False Negative values are calculated in order to analyze the performance of the system model. Table I shows the prototype of VCM. Table II shows the characteristics of VCM.

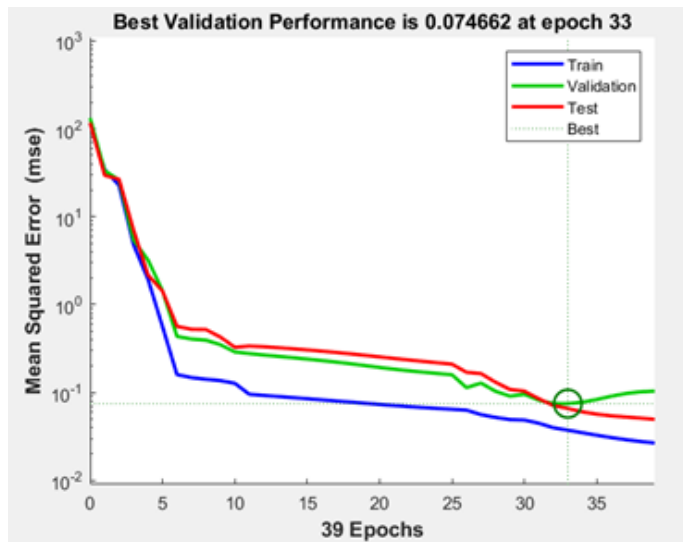


Fig. 3. Training Progress of the AED-HSR Model.

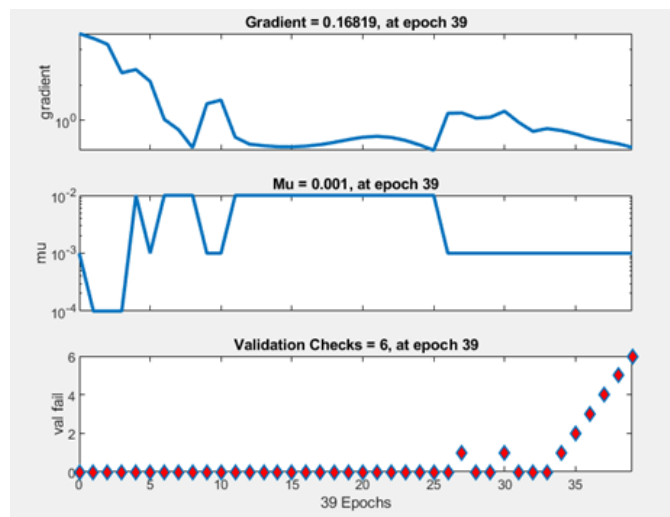


Fig. 4. Training State of the Proposed AED-HSR Model.

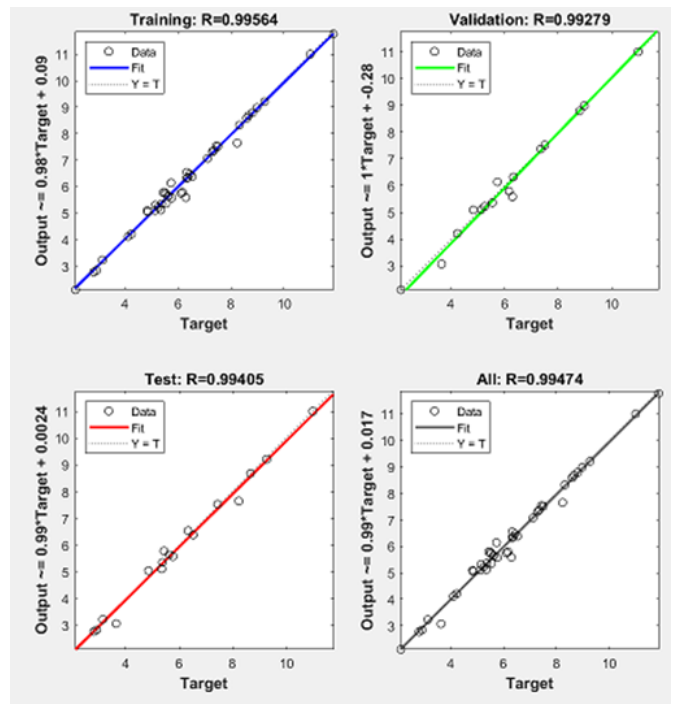


Fig. 5. Regression Plot of the Proposed AMSO-RNN Model.

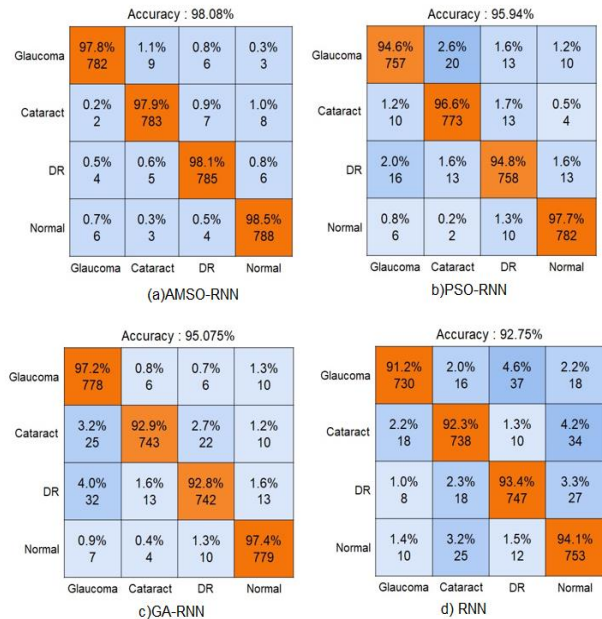


Fig. 6. Confusion Matrix of Four Different Methods.

TABLE I. VCM PROTOTYPE

		PREDICTED			
		X	Y	Z	R
ACTUAL	X	$L_{XX}$	$L_{XY}$	$L_{XZ}$	$L_{XR}$
	Y	$L_{YX}$	$L_{YY}$	$L_{YZ}$	$L_{YR}$
	Z	$L_{ZX}$	$L_{ZY}$	$L_{ZZ}$	$L_{ZR}$
	R	$L_{RX}$	$L_{RY}$	$L_{RZ}$	$L_{RR}$

TABLE II. CHARACTERISTICS OF VCM

<b>TRUE POSITIVE</b>	$TP_X = L_{XX}$
	$TP_Y = L_{YY}$
	$TP_Z = L_{ZZ}$
	$TP_R = L_{RR}$
<b>FALSE POSITIVE</b>	$FP_X = L_{YX} + L_{ZX} + L_{RX}$
	$FP_Y = L_{XY} + L_{ZY} + L_{RY}$
	$FP_Z = L_{XZ} + L_{YZ} + L_{RZ}$
	$FP_R = L_{XR} + L_{YR} + L_{ZR}$
<b>TRUE NEGATIVE</b>	$TN_X = L_{YZ} + L_{YY} + L_{ZY} + L_{YR} + L_{ZZ} + L_{RY} + L_{RZ} + L_{YR} + L_{RR}$
	$TN_Y = L_{XX} + L_{ZZ} + L_{XZ} + L_{XR} + L_{ZX} + L_{RR} + L_{RX} + L_{RZ} + L_{ZR}$
	$TN_Z = L_{RY} + L_{RR} + L_{XX} + L_{XY} + L_{XR} + L_{YX} + L_{YY} + L_{YR} + L_{RX}$
	$TN_R = L_{ZY} + L_{ZZ} + L_{XX} + L_{XY} + L_{XR} + L_{YX} + L_{YY} + L_{YZ} + L_{ZX}$
<b>FALSE NEGATIVE</b>	$FN_X = L_{XY} + L_{XZ} + L_{XR}$
	$FN_Y = L_{YX} + L_{YZ} + L_{YR}$
	$FN_Z = L_{ZX} + L_{XY} + L_{ZR}$
	$FN_R = L_{RX} + L_{RY} + L_{RZ}$

The proposed AED- HSR model detects the eye disease with an accuracy of 98.08%. DR detection from the proposed model is shown in Fig. 7. The classification of glaucoma using the proposed system model is shown in Fig. 8. Cataract image detection by utilizing the proposed AED-HSR model is shown in Fig. 9.

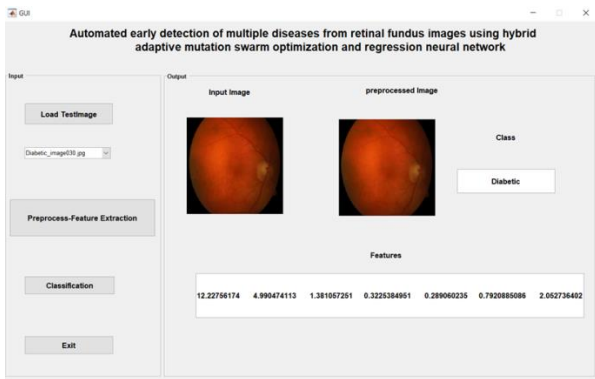


Fig. 7. Detection of DR.

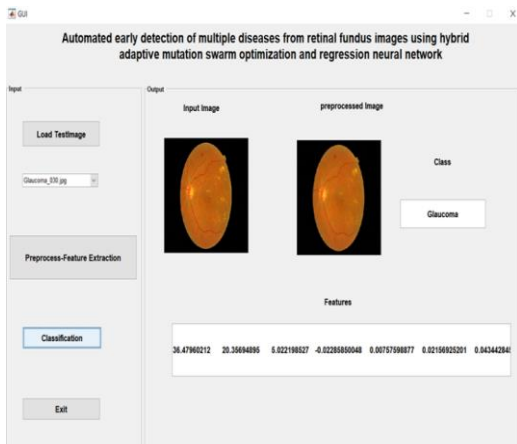


Fig. 8. Detection of Glaucoma.

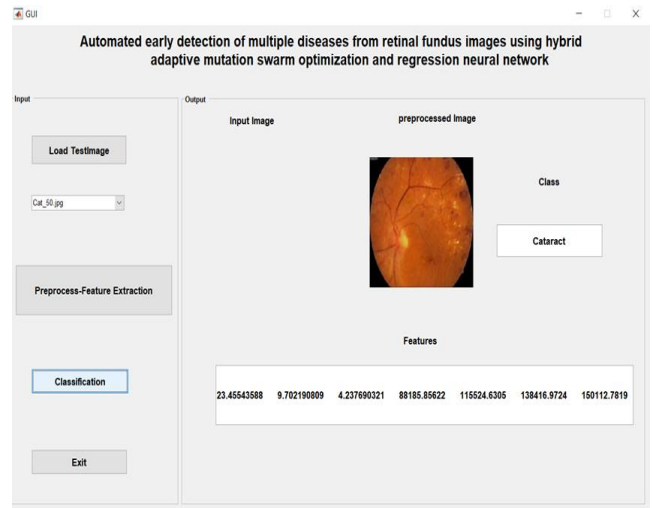


Fig. 9. Detection of Cataract.

### C. Performance Analysis

The proposed model performance can be analyzed in terms of accuracy, sensitivity, specificity, negative predictive value (NPV), positive predictive value (PPV), false negative rate (FNR), false positive rate (FPR), and false discovery rate (FDR) from VCM. Table III shows the parameters of the performance metrics. Sensitivity alludes to a test's capacity to assign a diseased image as positive. Specificity characterizes the capacity of the test to assign the non-diseased image as negative.

Accuracy is defined as the ratio of correctly predicted images to the total images. PPV refers to the probability that the individual has the disease when confined to those individuals who test positive. NPV measures the proportion of genuine negative expectations considering all negative forecasts. FNR is calculated by the ratio of false negative to total positive. The FDR measures the extent of the alerts that are irrelevant. Fig. 10 shows the performance metrics for each class of eye diseases based on RNN.

Fig. 10 shows that RNN has 94.1% accuracy rate for identifying the normal eyes. The maximum specificity for glaucoma affected eye is 98.5%. F1 score for DR is 95.41%.

TABLE III. PERFORMANCE METRICS PARAMETERS

Parameters	Formula
Sensitivity	$Sen = TP / (TP + FN)$
Specificity	$Spec = TN / (TN + FP)$ ;
Accuracy	$Acc = (TP+TN) / (TP+TN+FP+FN)$
False positive rate	$FPR = 1 - Spec$
False negative rate	$FNR = FN / (TP + FN)$
Positive predictive value	$PPV = TP / (TP + FP)$
Negative predictive value	$NPV = TN / (TN + FN)$ $NPV = TN / (TN + FN)$
False discovery rate	$FDR = 1 - PPV$
F1_Score	$F1\_Score = (2*TP) / ((2*TP) + FP + FN)$

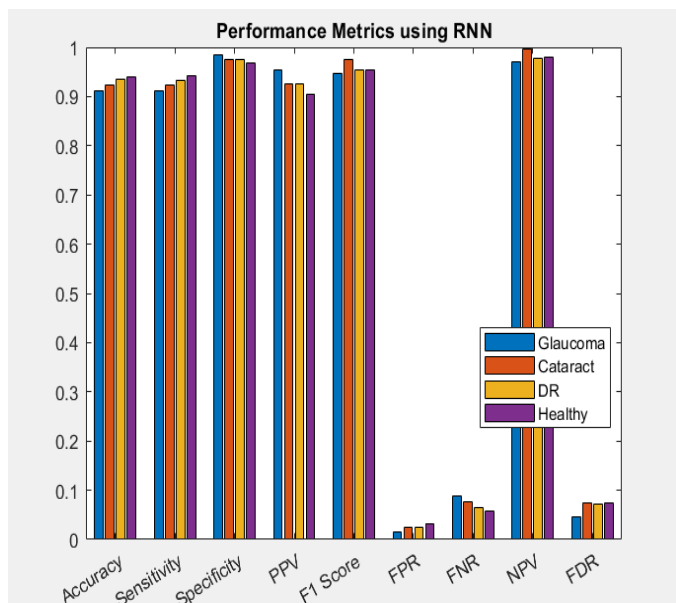


Fig. 10. Performance Metrics of each Class using RNN.

Fig. 11 indicates the performance metrics for each class of eye diseases based on GA-RNN. Fig.11 shows that GA-RNN has 97.4% accuracy rate for identifying the normal eyes. The maximum specificity for cataract affected eye is 99.04%. F1 score for Normal eye is 97.99%.

Fig. 12 indicates the performance metrics for each class of eye diseases based on PSO-RNN. Fig.13 shows that PSO-RNN has 97.7% accuracy rate for identifying the normal eyes. The maximum specificity for Normal eye is 98.87%. F1 score for Normal eye is 98.30%.

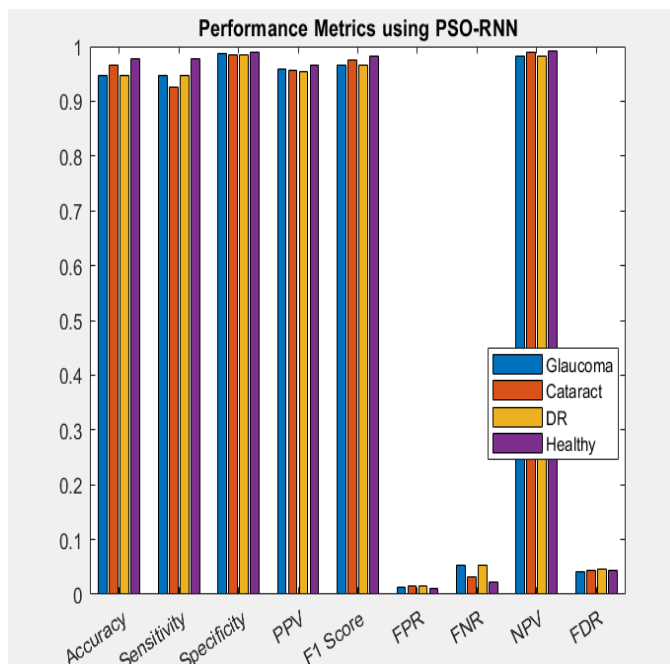


Fig. 12. Performance Metrics of each Class using PSO-RNN.

Fig. 13 indicates the performance metrics for each class of eye diseases based on the proposed AMSO-RNN. Fig. 13 shows that AMSO-RNN has 98.5 % accuracy rate for identifying the normal eyes. The maximum specificity of Glaucoma diseased eye is 99.5% F1 score for Normal eye is 98.83%.

Overall, the system automatically detects the eye disease with 98.08 % accuracy, 99.34% specificity, 98.03% sensitivity, 98.03% PPV, 99.34% NPV, 0.62% FPR, 1.93% FNR, 98.67% F1 Score and 1.96% FDR.

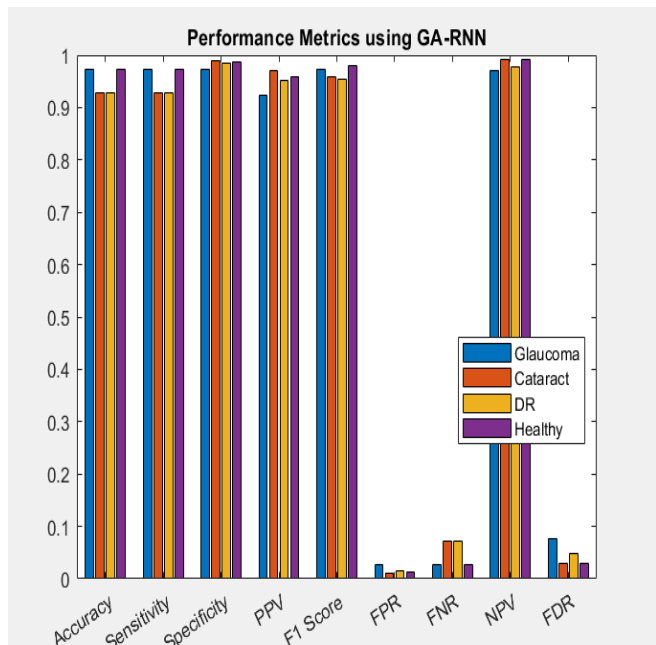


Fig. 11. Performance Metrics of each Class using GA- RNN.

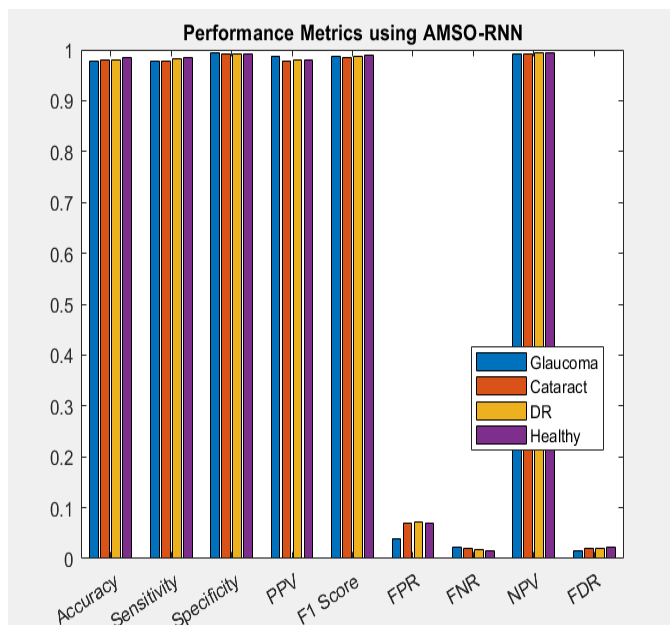


Fig. 13. Performance Metrics of each Class using AMSO-RNN.

The performance Matrix of AMSO-RNN is compared with that of the other strategies, namely RNN-PSO, RNN-GA, and RNN, as shown in the Fig. 14. From the comparison measures of four different methods, the proposed method has an improvement of 2.23% in accuracy, 2.18% in sensitivity, 0.71% in specificity, 2.19% increase in PPV, 1.45% increase in F1 Score, 53.38% decrease in FPR, 51.99% decrease in FNR, 0.72% increase in NPV and 54.2% decrease in FDR when compared with RNN-PSO. Also, the proposed AMSO-RNN provides an improvement of 3.16 % in accuracy, 3.14% in sensitivity, 1.01% in specificity, 3.08 % increase in PPV, 2.09% increase in F1 Score, 61.73% decrease in FPR, 60.61% decrease in FNR, 1.01% increase in NPV and 58.69% decrease in FDR when compared with RNN-GA and an improvement of 5.75% in accuracy, 5.72% in sensitivity, 1.88% in specificity, 5.68% increase in PPV, 3.79% increase in F1 Score, 74.05% decrease in FPR, 73.27% decrease in FNR, 1.83% increase in NPV and 70.61% decrease in FDR when compared with RNN.

**D. Comparison of Proposed Method with Previous Studies**

This subsection details the performance analysis comparison of the proposed method with other state of art methods. Table IV shows the performance comparison of the proposed method with previous strategies.

TABLE IV. COMPARISON OF PROPOSED METHOD WITH PREVIOUS STUDIES

Author	Task	Method	Accuracy (%)	Sensitivity (%)	Specificity (%)	F-1 Score (%)
Oh et al. [20]	DR	ETDRS&SF	83.38	80.6	83.41	-
Latif et al. [28]	Glaucoma	ODG-NET	95.75	94.90	94.75	-
AZhar et al. [32]	Cataract	CNN - SVM	95.6	-	-	-
Tayal et al [39]	DME, Drusen, Choroidal, Normal	DL-CNN	96.5	-	98.6	-
Proposed method	Glaucoma DR, Cataract, Normal	AMSO-RNN	98.08	98.03	99.34	98.67

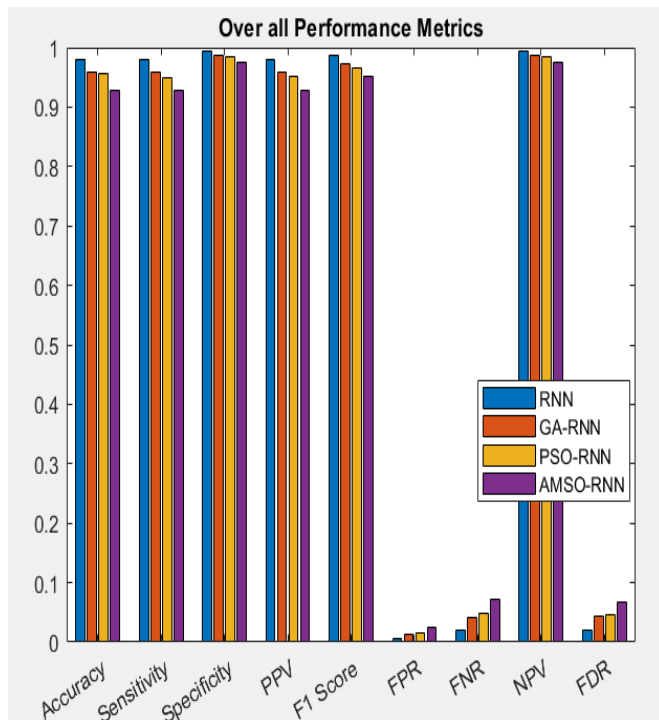


Fig. 14. Overall Performance Metrics.

**V. CONCLUSION**

From retinal fundus images, the proposed AED-HSR technique automatically detects the types of different eye diseases such as DR, glaucoma, and cataract from the retinal fundus images. In this approach, the input images are preprocessed by masking, thresholding, and resizing. The resized image is denoised by using gray level morphological transformation. The preprocessed image is then subjected to feature extraction in order to retrieve the image's statistical features. The collected features are then segmented using AMSO and given to the RNN Classifier. The proposed algorithm has been tested on an ODIR database from the Kaggle datasets. The proposed system predicts the type of the disease with 98.08% accuracy, 99.34% specificity, 98.03% sensitivity, 98.03% PPV, 99.34% NPV, 0.62% FPR, 1.93% FNR, 98.67% F1 Score and 1.96% FDR. The proposed methods provide better results in contrast with the other techniques such as RNN-PSO, RNN-GA, and RNN. The model that has been proposed provides better performance metrics when compared with the other networks in terms of accuracy, specificity, sensitivity, PPV, NPV, FPR, FNR, FNR, F1Score and FDR. The outcome of this study points to the enhancement of the suggested network architecture as work that should be done in order to achieve future improvements in terms of performance.

REFERENCES

- [1] Centers for disease control and prevention: <https://www.cdc.gov/visionhealth/basics/ced/index.html>.
- [2] Adapa D, Joseph Raj AN, Alisetti SN, Zhuang Z, K. G, Naik G, (2020) .A supervised blood vessel segmentation technique for digital Fundus images using Zernike Moment based features.PLoS ONE 15(3),[tps://doi.org/10.1371/journal.pone.0229831](https://doi.org/10.1371/journal.pone.0229831).
- [3] P. Costa, A. Galdran, A. Smailagic and A. Campilho, (2018). A Weakly-Supervised Framework for Interpretable Diabetic Retinopathy Detection on Retinal Images, in IEEE Access, vol. 6, pp. 18747-18758, doi: 10.1109/ACCESS.2018.2816003.
- [4] S. Kumar and B. Kumar, (2018) Diabetic Retinopathy Detection by Extracting Area and Number of Microaneurysm from Colour Fundus Image, 2018 5th International Conference on Signal Processing and Integrated Networks (SPIN), Noida,pp.359-364, doi: 10.1109/SPIN.2018.8474264.
- [5] N. H. Harun, Y. Yusof, F. Hassan and Z. Embong, (2019). Classification of Fundus Images For Diabetic Retinopathy using Artificial Neural Network, 2019 IEEE Jordan International Joint Conference on Electrical Engineering and Information Technology (JEEIT), Amman, Jordan, pp. 498-501, doi: 10.1109/JEEIT.2019.8717479.
- [6] S. Ekapture and R. Jain, (2018). Red Lesion Detection in Digital Fundus Image Affected by Diabetic Retinopathy,2018 Fourth International Conference on Computing Communication Control and Automation (ICCUBEA), Pune, India, pp. 1-4, doi: 10.1109/ICCUBEA.2018.8697387.
- [7] N. Karami and H. Rabbani (2017). A dictionary learning based method for detection of diabetic retinopathy in color fundus images, 2017 10th Iranian Conference on Machine Vision and Image Processing (MVIP), Isfahan,, pp. 119-122.
- [8] L. Qiao, Y. Zhu and H. Zhou,Diabetic,(2020). Retinopathy Detection Using Prognosis of Microaneurysm and Early Diagnosis System for Non-Proliferative Diabetic Retinopathy Based on Deep Learning Algorithms, in IEEE Access, vol. 8, pp. 104292-104302, doi: 10.1109/ACCESS.2020.2993937.
- [9] P. Lopes, A. Ribeiro and C. A. Silva, (2019). Dilated Convolutions in Retinal Blood Vessels Segmentation, 2019 IEEE 6th Portuguese Meeting on Bioengineering (ENBENG), Lisbon, Portugal, pp. 1-4, doi: 10.1109/ENBENG.2019.8692520.
- [10] E. Sutanty, D. A. Rahayu, Rodiah, D. T. Susetianingti and S. Madenda,( 2017). Retinal blood vessel segmentation and bifurcation detection using combined filters, 2017 3rd International Conference on Science in Information Technology (ICSITech), Bandung, pp. 563-567,doi:10.1109/ICSITech.2017.8257176.
- [11] Preethy Rebecca, P. Allwin, S. (2021). Detection of DR from retinal fundus images using prediction ANN classifier and RG based threshold segmentation for diabetes. J Ambient Intell Human Comput 12, 10733–10740 doi.org/10.1007/s12652-020-02882-3.
- [12] Kalyani, G., Janakiramaiah, B., Karuna, A. et al. (2021).Diabetic retinopathy detection and classification using capsule networks. Complex Intell. Syst. <https://doi.org/10.1007/s40747-021-00318-9>.
- [13] Bhardwaj, C., Jain, S. & Sood, M. (2021). Hierarchical severity grade classification of non-proliferative diabetic retinopathy. J Ambient Intell Human Comput 12, 2649–2670 <https://doi.org/10.1007/s12652-020-02426-9>.
- [14] Mansour, R.F., Al-Marghilnai, A. (2021) .Glaucoma detection using novel perceptron based convolutional multi-layer neural network classification. Multidim Syst Sign Process 32, 1217–1235. <https://doi.org/10.1007/s11045-021-00781-0>.
- [15] Ajesh, F., Ravi, R. & Rajakumar, G. (2021). Early diagnosis of glaucoma using multi-feature analysis and DBN based classification. J Ambient Intell Human Comput 12, 4027–4036. <https://doi.org/10.1007/s12652-020-01771-z>.
- [16] Rutuja Shinde, ,(2021) Glaucoma detection in retinal fundus images using U-Net and supervised machine learning algorithms, Intelligence-Based Medicine, 5 100038, <https://doi.org/10.1016/j.ibmed.2021.100038>.
- [17] H. Wu, J. Lv and J. Wang, (2021)Automatic Cataract Detection with Multi-Task Learning,2021 International Joint Conference on Neural Networks (IJCNN), pp. 1-8, doi: 10.1109/IJCNN52387.2021.9533424.
- [18] M. R. Hossain, S. Afroz, N. Siddique and M. M. Hoque, (2020), Automatic Detection of Eye Cataract using Deep Convolution Neural Networks (DCNNs), 2020 IEEE Region 10 Symposium (TENSYP), pp. 1333-1338.
- [19] T. S. Mulati and F. Utamingrum, (2021) Hidden Neuron Analysis for Detection Cataract Disease Based on Gray Level Co-occurrence Matrix and Back Propagation Neural Network, 2021 International Conference on ICT for Smart Society (ICISS), pp. 1-5, doi: 10.1109/ICISS53185.2021.9533263.
- [20] Oh, K., Kang, H.M., Leem, D. et al. (2021). Early detection of diabetic retinopathy based on deep learning and ultra-wide-field fundus images. Sci Rep 11, 1897 <https://doi.org/10.1038/s41598-021-81539-3>.
- [21] Saeid Jafarzadeh Ghouschi, Ramin Ranjbarzadeh, Amir Hussein Dadkhah, Yaghoub Pourasad, Malika Bendechache, (2021),An Extended Approach to Predict Retinopathy in Diabetic Patients Using the Genetic Algorithm and Fuzzy C-Means, BioMed Research International, , <https://doi.org/10.1155/2021/5597222>.
- [22] Ai Zhuang, Huang Xuan, Fan Yuan, Feng Jing, Zeng Fanxin, Lu Yaping Detection Algorithm of Diabetic Retinopathy Based on Deep Ensemble Learning and Attention Mechanism Frontiers in Neuroinformatics 15, 2021, DOI=10.3389/fninf.2021.778552, ISSN=1662-5196.
- [23] Rego S, Dutra-Medeiros M, Soares F, Monteiro-Soares M, (2021), Screening for Diabetic Retinopathy Using an Automated Diagnostic System Based on Deep Learning: Diagnostic Accuracy Assessment. Ophthalmologica ,pp250-257.
- [24] Mohammedhasan, M., Uğuz, H. (2020),A new early-stage diabetic retinopathy diagnosis model using deep convolutional neural networks and principal component analysis. Traitement du Signal, 37, 711-722. <https://doi.org/10.18280/ts.370503>.
- [25] Hemelings, R., Elen, B., Barbosa-Breda, J. et al. (2021). Deep learning on fundus images detects glaucoma beyond the optic disc. Sci Rep 11, 20313 <https://doi.org/10.1038/s41598-021-99605-1>.
- [26] Salam, A.A., Khalil, T., Akram, M.U. et al. (2016).Automated detection of glaucoma using structural and nonstructural features. Springer Plus 5, 1519 <https://doi.org/10.1186/s40064-016-3175-4>.
- [27] Nataraj Vijapur, & R. Srinivasa Rao Kunte, (2020) . Efficient Machine Learning Techniques to Detect Glaucoma using Structure and Texture based Features. International Journal of Recent Technology and Engineering (IJRTE), 9 ,pp.193–201.
- [28] Latif, J., Tu, S., Xiao, C. et al. (2022). ODGNet: a deep learning model for automated optic disc localization and glaucoma classification using fundus images. SN Appl. Sci. 4, 98 ,<https://doi.org/10.1007/s42452-022-04984-3>.
- [29] Xu, X., Guan, Y., Li, J. et al. (2021),Automatic glaucoma detection based on transfer induced attention network. BioMed Eng OnLine 20, 39. <https://doi.org/10.1186/s12938-021-00877-5>.
- [30] Raja, J., Shanmugam, P. & Pitchai, R. (2021) An Automated Early Detection of Glaucoma using Support Vector Machine Based Visual Geometry Group 19 (VGG-19) Convolutional Neural Network. Wireless Pers Commun 118,pp. 523–534.
- [31] Md Kamrul Hasan, Tanjum Tanha, Md Ruhul Amin, Omar Faruk, Mohammad Monirujjaman Khan, Sultan Aljahdali, Mehedi Masud, (2021),Cataract Disease Detection by Using Transfer Learning-Based Intelligent Methods, Computational and Mathematical Methods in Medicine, Article ID 7666365, 11 pages .
- [32] Azhar Imran, Jianqiang Li, Yan Pei, Faheem Akhtar, Ji-Jiang Yang & Yanping Dang,(2020) . Automated identification of cataract severity using retinal fundus images, Computer Methods in Biomechanics and Biomedical Engineering: Imaging & Visualization, 8:6, pp. 691-698, DOI: 10.1080/21681163.2020.1806733.
- [33] T. Pratap and P. Kokil, (2019).Automatic Cataract Detection in Fundus Retinal Images using Singular Value Decomposition,2019 International Conference on Wireless Communications Signal Processing and Networking (WiSPNET), pp. 373-377, doi: 10.1109/WiSPNET45539.2019.9032867.

- [34] A. Imran, J. Li, Y. Pei, F. Akhtar, J. -J. Yang and Q. Wang, (2019), Cataract Detection and Grading with Retinal Images Using SOM-RBF Neural Network, 2019 IEEE Symposium Series on Computational Intelligence (SSCI), pp. 2626-2632.
- [35] M. K. Behera, S. Chakravarty, A. Gourav and S. Dash, (2020), Detection of Nuclear Cataract in Retinal Fundus Image using Radial Basis Function based SVM, 2020 Sixth International Conference on Parallel, Distributed and Grid Computing (PDGC), pp. 278-281, doi: 10.1109/PDGC50313.2020.9315834.
- [36] F. A. Hashim, N. M. Salem and A. F. Seddik, (2013). Preprocessing of color retinal fundus images, 2013 Second International Japan-Egypt Conference on Electronics, Communications and Computers (JEC-ECC), 6th of October City, pp. 190-193, doi: 10.1109/JEC-ECC.2013.6766410.
- [37] Lamia Abed Noor Muhammed, Localizing Optic Disc in Retinal Image Automatically with Entropy Based Algorithm, International Journal of Biomedical Imaging, (2018) Article ID 2815163, 7 pages, doi.org/10.1155/2018/2815163.
- [38] Zafer Yavuz, Cemal Köse, (2017). Blood Vessel Extraction in Color Retinal Fundus Images with Enhancement Filtering and Unsupervised Classification, Journal of Healthcare Engineering, Article ID 4897258, 12 pages, doi.org/10.1155/2017/4.
- [39] Tayal, A., Gupta, J., Solanki, A. et al. (2021). DL-CNN-based approach with image processing techniques for Diagnosis of retinal diseases. Multimedia Systems. <https://doi.org/10.1007/s00530-021-00769-7>.